Characterization of historical earthquakes through a study of landslides by lichenometry (Murcia, SE Iberia)

Cristina Crespo-Martín[a*], José Jesús Martínez Díaz[b,c], Fidel Martín-González[a]

[a] ESCET Área de Geología. Tecvolrisk Research Group. Universidad Rey Juan Carlos. C/Tulipán s/n, Móstoles, 28933, Madrid, Spain.
[b] Department of Geodynamics, Stratigraphy and Paleontology, Universidad Complutense de Madrid. C/Jose Antonio Novais 12, 28040, Madrid, Spain.
[c] IGEO Geosciences Institute (UCM-CSIC), 28040, Madrid, Spain.

* Corresponding author. E-mail address: cristina.crespo@urjc.es (C. Crespo-Martín).

ORCID: https://orcid.org/0000-0002-8755-9784, https://orcid.org/0000-0002-5239-1846, https://orcid.org/0000-0003-4846-0279

ABSTRACT

Earthquakes with magnitudes greater than 4.5-5 induce massive rockfalls close to the fault rupture zone. Driven by seismic shaking, the blocks collapse through the hillslope, which yields a fresh surface that is unbeatable for new lichen colonization. The lichenometric technique involves dating lichens developed on the surfaces of rockfall blocks induced by earthquakes. This study is focused on Cejo de Cano (Lorca, Spain), which is an earthquake-prone landslide scarp, as shown after the 2011 Lorca shaking (Mw 5.2). After this event, the possibility that the rocky volume at the foot of its slope could have a seismic origin started to be considered. In this research, lichenometry is used to date lichens on rock surfaces and test a possible correlation with the cataloged historical earthquakes. This research is important because of the large number of rockfall earthquakes found at this site by applying lichenometry compared to other studies in the literature. This technique allows us to extend the regional seismic catalog because the oldest lichens are older than the documented catalog of historical earthquakes. An oriented rockfall pattern that correlates with the location of epicenters is observed. In addition, the parallel and oblique previous fracturing of Cejo de Cano makes this scarp a suitable place to test whether the fracturing direction of the scarp could control a greater volume of rockfalls. This research opens up a new field of study to evaluate this correlation in larger areas.

Keywords: lichens, rockfall, fracturing, pattern, Lorca, seismicity

1. INTRODUCTION

Earthquakes are one of the major causes of landslides around the world, which in turn represent one of the more significant hazards associated with earthquakes in mountainous regions (Harp and Jibson 2002; Morzoratia et al. 2002; Koukouvelas et al. 2015; Li et al. 2022). Moreover, population increase and new settlements cause that the landslides generate greatly impact on the seismic hazards in these regions, blocking road transportation, disrupting rescue lines, etc. (Bommer and Rodríguez 2002; Khazai and Sitar

2003; Lin et al. 2003). The basis of seismic hazard studies is formed by analyzing earthquakes that happened in a region by completing seismic catalogs (Musson 1996; Guidoboni and Ebel 2009). Seismic catalogs provide information on past events and their coseismic effects, such as landslides or earthquake damage to buildings, which provide information about ground shaking, intensity, etc. (e.g., Korjenkov and Mazor 1999; Guidoboni and Ebel 2009, 2013; Udías 2015; Martin-González 2018; Crespo-Martin et al. 2018). The completeness of data in historical catalogs with these seismic parameters is essential to provide better insights into earthquake recurrence, intensity, and location and to evaluate seismic hazards and building requirements. Therefore, studies of landslide characteristics associated with specific earthquakes can be of great interest for seismic catalog completeness (Brune 1996; Bull 2003). Moreover, landslides have preferred orientations and distributions (e.g., Sato et al. 2007; Meunier et al. 2013; Xu et al. 2014). Seismogenic fault parameters, such as trends and kinematics, are some of the controls on landslide spatial patterns (Meunier et al. 2013; Delano et al. 2018; Martino et al. 2022). Studies of these spatial patterns can constrain and shed light on seismogenic faults (Delano et al. 2018; Martín-González 2021). However, studies of ancient landslides are complex due to the difficulty of assigning them to specific events.

Lichenometry is a technique used to date rockfalls induced by historical earthquakes. The blocks fall down the hillslope because of seismic shaking; they bounce and roll along the ground and provide a fresh surface that is ideal for new lichen colonization (Bull 2003). Lichenometry is suitable for dating not only large earthquakes involving surface ruptures but also moderate earthquakes that induce significant ground shaking. Lichenometric dating of coseismic landslides was initially performed in the Southern Alps in New Zealand (Bull 1996b; Bull and Brandon 1998) and for earthquakes associated with the San Andreas Fault in California (Bull 1996a). In the Iberian Peninsula, coseismic rockfalls in the well-known 1755 Lisbon earthquake and the SE Iberia earthquakes have also been dated (Pérez López et al. 2012a, 2019).

The study area selected for this research is a scarp composed of limestones and calcarenites, named *Cejo de Cano*, located in the seismic area of the western Murcia region, 10 km to the NW of Lorca (Eastern Betic Cordillera, Spain). The interest in this site is based on the following: 1.- it is a scarp prone to rockfalls induced by moderate earthquakes, 2.- more than 12 earthquakes recorded in the seismic catalog with intensities >V occurred within a distance < 40 km, and 3.- the scarp has a wide range of orientations that allow to record different ground motion senses. Several seismic-induced rockfalls were produced in the region, including that in the 2011 Lorca earthquake, which suggests the high potential of this region to undergo this phenomenon (Alfaro et al. 2012; Delgado et al. 2020; Rodríguez-Peces et al. 2020). Among the earthquakes in the study region, it is remarkable that the 2011 Lorca earthquake, despite its moderate magnitude (Mw 5.2 ESI07 VI-VII), induced relevant coseismic geological effects, including a remarkable volume of material mobilized by rockfalls (Alfaro et al. 2012; Pérez-López et al. 2012b; Rodríguez-Peces et al. 2012; Rodríguez-Peces et al. 2020), as well as events in other regions (Guemache et al. 2010). Because of the descriptions of historical earthquake effects and the 2011 earthquake, earthquakes with magnitudes greater than 4.5-5 have generated massive rockfalls close to the fault rupture zone and up to more than 12 km away (Rodríguez-Peces et al. 2014; Guemache et al. 2010).

The aims of this study are as follows: 1.- verify the seismic origin of the rockfalls observed in the studied scarp and assign and identify specific rockfall volumes to historical events recorded in the historical catalog. Using this technique, nonrecorded events are identified, which complete the regional seismic catalog, not only for large earthquakes but also for moderate earthquakes. 2.- The second aim is to analyze the characteristic rockfall pattern. 3.- The last aim is to verify whether the orientations of the fracture systems existing in the rock that forms the scarp control the directions of rockfalls along the Cejo de Cano. This study sheds light on earthquake-induced rockfalls and establishes a relation between historical earthquakes and rockfall patterns, which can be helpful for disaster management, rehabilitation, and risk mitigation for future earthquakes.

2. GEOLOGICAL AND SEISMOLOGICAL FRAMEWORK

2.1. GEOLOGICAL AND STRUCTURAL SETTING

The Cejo de Cano is a 6 km-long scarp located 10 km to the NW of Lorca and the Eastern Betic Shear Zone in the SE of the Betic Cordillera. This area is located close to the boundary between the Eurasian and Nubian plates. It is characterized by the existence of a high density of neotectonic faults and fractures: normal faults with orientations ranging from NW–SE to NNE–SSW and strike-slip and oblique-slip faults with orientations ranging from NE–SW to E–W (Martínez-Díaz et al. 2012a, 2012b).

(POSITION OF FIGURE 1)

The Cejo de Cano, near the Puentes reservoir, is located on the NW edge of the Miocene Lorca Basin. This basin is bounded by the mountain ranges of Sierra de Peña Rubia to the south, Sierra de la Tercia to the southeast, and Sierra de Espuña to the northeast, and by the Betic external zones to the northwest (Fig. 1). The sedimentary record started in the Serravallian–Tortonian transition as a result of tectonic activity that induced relative vertical movements of different tectonic blocks (Guillén-Mondéjar et al. 1995). Cejo de Cano is a prominent morphological scarp-oriented NNE–SW to NE–SW and formed by late Tortonian marine deposits. It is controlled by a strong lithological and mechanical contrast between the resistant strata of limestones and calcarenites to the east and marls and alluvial deposits to the west (Fig. 2). The calcarenite and limestone layers dip gently to the E and SE, generating the rocky cliffs under study, with heights ranging from 511 to 586 m (Figs. 1 and 2).

The orientation and structure of the scarp are controlled by a system of normal and oblique normal–strike slip faults oriented NNE–SSW, NE–SW, and NE–SW (Guillén-Mondéjar 1994; Martínez Díaz 1999). These fault sets affect the rocks in the scarp at several scales (from metric to kilometric sizes) and control the orientations of the scarp segments, orientations of the rockfalls, and volume of the rock blocks that appear at the foot of the scarp.

(POSITION OF FIGURE 2)

The most active fault in the region is the Alhama de Murcia Fault (AMF), which has oblique sinistral–reverse kinematics and a NE–SW orientation. It is the largest active fault in the Eastern Betic Shear Zone (Silva et al. 1993; Martínez-Díaz et al. 2012a). GPS velocity data suggest that this fault has a velocity of stress load of 1.5±0.3 mm/a (Echeverría et al. 2013), which is faster in the Iberian Peninsula. In addition, paleoseismic studies on the AMF showed that seismic events with magnitudes greater than 6.5 occurred during the Holocene (Ortuño et al. 2012). According to the Quaternary Active Faults Database of Iberia, other smaller active faults are located less than 20 km away from Cejo de Cano, such as the E–W and NW–SE Las Viñas fault to the south of the scarp, the NNW–SSE Llano de las Cabras fault to the NE of the scarp and the West of Pericay–Gigantes fault in the NW sector of the scarp (IGME 2023).

2.2. HISTORICAL SEISMICITY IN THE REGION

Historically, the most destructive earthquakes (e.g., 1579, 1674, 1818 and 1907) in the study area are located close to Lorca and associated with the Alhama de Murcia Fault (Martínez-Díaz et al. 2012b). Before the last destructive 2011 earthquake, several damaged historical earthquakes with high intensities were known to have affected the Lorca region (Table 1 and Fig. 1) (Martínez-Solares and Mezcua Rodríguez 2002).

(POSITION OF TABLE 1)

The data of historical and instrumental earthquakes in the vicinity of the study region are collected from the Spanish National Seismic Network (Table 1) (IGN 2023). For the analysis, historical earthquakes are selected in a radius of 40 km and intensity (EMS-98) ≥ IV, as they could affect the study region with enough intensity to provoke rockfalls (Rodríguez-Peces et al. 2014).

Considering the described conditions of intensity and proximity to the studied scarp, twelve historical earthquakes are analyzed; nine earthquakes were registered at Lorca, two events were recorded at Totana and one earthquake was recorded at Librilla (Table 1 and Fig. 1). Distances and orientations of earthquakes are given based on the Cejo de Cano. The earthquakes are as follows:

1.- Lorca earthquakes 1579, 1674, 1713, and 1783. Located 10-12 km to the SE. The two larger earthquakes were the 1579 event that shook the region with an EMS intensity of VII and the 1674 earthquake with a higher intensity (VIII EMS).

2.- Lorca 1818 earthquake (VI-VII EMS). Located 13 km to the east.

3.- Librilla 1855 earthquake (VI-VII EMS). Located 40 km to the ENE.

4.- Totana 1872 (IV-V EMS). Located to 20 km to the east.

5.- Totana 1907 earthquake (VII EMS). Located 25 km to the ENE.

6.- Lorca 1932 earthquake (V EMS). Located 12 km to the SE.

7.- Lorca 1963 earthquake (V EMS). Nearest event (9 km); located WNW.

8.- Lorca 1977 earthquake (VI EMS). Located 14 km to the SSE.

9.- Lorca 2011 earthquake (VII EMS). Located to 9 km to the ESE.

Even the high-intensity (VII) event, which is located within 30 km and is within temporal proximity of the 1932 earthquake in Lorca, allows us to exclude the 1948 Cehegín earthquake from this study due to a possible overlapping temporal effect.

It is worth noting a far-field earthquake that could have affected the locality. The 1755 Cabo de San Vicente earthquake, better known as the Lisbon earthquake of 1755, has left evidence of rock mass mobilization in the *Rambla de los 17 Arcos* within the municipality of Lorca, as well as 70 km northeast of the study region, and therefore could also have caused rockfalls in the study area (Pérez-López et al. 2012a, 2019).

3. METHOD

Lichenometry is a dating technique that is often used to quantify variations in the exposures of rock surfaces and morphologies, such as moraines, rock glaciers, landslide deposits or rockfalls, because of the estimation of the relative growth of the lichens developed on the surfaces (Chueca-Cía 1991). Several lichenometric dating studies measure the historical movement and activity of glacial moraines around the world: in the Andes, specifically in Argentina (Garibotti and Villalba 2009), in the Jotunheimen Mountains in southern Norway (Matthews 2005) or in the rocky glacier of Skjoldalur in Iceland (Chueca-Cía 1991). An example of lichenometric dating in landslide deposits is a study in the Alta Ribagorza in the Eastern Oscense Pyrenees (Chueca-Cía and Julián-Andrés 1995).

Numerous studies have revealed that during strong earthquakes, massive rockfalls are generated, and new rupture surfaces are colonized by lichens (Bull et al. 1994; Harp and Jibson 1996; Pérez-López et al. 2012a). Lichenometry of coseismic rockfalls was developed after discovering that the growth of lichens on rocky slopes affected by earthquakes records pulses of rockfalls related to historical earthquakes (Bull 1996a; Bull and Brandon 1998). Some ancient rockfalls are also observed in nearby regions, and they relate to the described historical events, such as the 1674 Lorca earthquake or the far-field Lisbon earthquake in 1755 (Table 1) (Pérez-López et al. 2012a). As a result of the 2011 Lorca earthquake, it was shown that shallow strike-slip earthquakes (even in cases of low magnitude such as this Mw 5.2 event) tend to promote processes of directivity in rupture propagation, which could provoke pulses of stronger ground motion normal to the fault plane. These effects could be relevant in controls on the volume of rockfalls in areas close to the causative faults (Alfaro et al. 2012; Martínez-Díaz et al. 2012a; Rodríguez-Peces et al. 2012).

Dating and locating preinstrumental earthquakes using lichenometry is a challenge, and the careful selection of blocks is essential. Rockfall-prone sites, including steep slopes, glacial moraines, alluvial fans, and even meteorological events, favor the addition of new blocks to slopes (Benedict 1967; Bull 1996a). All scarps are formed by the same lithology (Fig. 1b), which provides lichens with the same growth conditions. The wide variation in the scarp orientation and three main orientations of segments (N–S, NNE–SSW, and NE–SW) make the Cejo de Cano an optimal place to test rockfall orientation patterns (Fig. 1a). In addition, the sample sites were thoroughly and carefully selected to reduce factors influencing lichen growth rates (e.g., humidity variations and shadows caused by trees) (Porter 1981; Bull et al. 1994). Due to the lack of trees on the selected scarp, the collection of lichenometric data avoids the problem of irregular light conditions.

The scarp is only 4.8 km in length, and all the studied segments are affected by homogeneous climatic and meteorological conditions, reducing the probability of uneven lichen growth. Moreover, lichens are strictly measured on horizontal surfaces to avoid different growth rates, depending on the orientation of the surface. The resemblance of these characteristics throughout the scarp, which indicates similar growth conditions, makes it an ideal site for lichenometric analysis.

For lichenometric analysis, crustose lichens with discoidal geometry are frequently used, as they are characterized as isolated individuals whose food base is the rock; they are regularly disc-shaped and have constant growth throughout their life (Jomelli et al. 2007; Pérez-López et al. 2012a). The lithologies present in Cejo de Cano are calcarenites, limestones, and calcareous sandstones, so the lichens that are used are crustose calcareous lichens associated with temperate climates (Fig. 2b) (Pérez-López et al. 2012a, 2019). In this study, the species selected for dating is the crustose calcareous lichen *Aspicilia calcarea*, which has a discoidal geometry with a grayish white thallus (Rogers, 1999) (Fig. 3d). It is associated with carbonate rocks in sunny areas and temperate climates and is very common in the Mediterranean region and specifically in SE Spain (Hughes 2007; Pérez-López et al. 2012b).

(POSITION OF FIGURE 3)

The research of McCarthy and Smith (1995) points out the importance of calibrating a regional growth curve for each lichen since its growth is conditioned by the hours of light, precipitation, lithology, and other local factors. Because of this calibration, it is possible to estimate the exposure age of the rock surface and to relate the diameter of the lichen to the time of its colonization. The calibration curve applied in this study is based on the previous research of Pérez-López et al. (2012a), which calibrated the mean annual growth rates using local lichens. They measured lichens on subhorizontal surfaces (inclinations less than 15°) to avoid several orientations and sunstroke hours that could affect a homogenous annual rate of thallus growth. The curve is calibrated using lichen diameters in historical buildings, cemetery graves, and monuments of known age, with identical lithologies and environmental conditions. The mean annual growth rate determined in the city of Lorca for *Aspicilia calcarea* is 0.235 mm/year (Pérez-López et al. 2012a). The mean annual growth rate was estimated based on the lichen of largest diameter, measured in monuments of known age (aqueduct of *Rambla de los 17 Arcos* of 1791).

Measurements of the thallus diameter of *Aspicilia calcarea* are made with a digital caliper and based on the longest-diameter approach (Winchester 2023). Considering that the data were collected in 2015, the calendar age is the year 2015 minus the lichen age. A temporal range of ecesis of 10 years is used, i.e., the lichens start to colonize the surface within a period of 10 years after the rockfall event (Wilkinson 2011). A prior study indicates that for the largest-lichen approach, it is possible to observe a rapid sigmoidal growth rate during the first 31 years (in the case of Aspicilia calcarea) followed by decline to low constant growth (Winchester 1984; 2023). In this study, only 2% of lichen measurements could be affected; therefore, this phenomenon is considered to have an insignificant influence on the results and discussion of this research.

The different orientations of the segments that draft the Cejo de Cano scarp suppose that by measuring the orientation of the fracture families present in the rock that forms the scarp, whether the angle between the fractures and the scarp has a significant influence on the volume of material involved in the rockfalls is studied. The orientations of minor faults and fractures were measured in the field along each segment, and hectometric faults were measured using aerial images.

To estimate the total displaced rock volume, an DTM (Digital Terrain Model) of the studied region with a horizontal resolution of 2 m and vertical resolution of 25 cm obtained with LIDAR raw data from the IGN is used. It also utilizes 25 cm-resolution orthophotography. After digitalization of the map view section of each block using GIS, a spherical shape is assumed for each block, and the volumes of all blocks are added to estimate the total volume mobilized per segment.
The assessment of the volume of dislodged blocks per segment and the main fracturing direction of each allows us to test the relation between both factors.

4. RESULTS

It is possible to divide the scarp into 22 segments according to their orientation. These segments are classified into Groups A, B, and C, following the orientation ranges of 0°-32°, 56°-97°, and 97°-150°, respectively (Table 2) (Figs. S.1 to S.4).

(POSITION OF TABLE 2)

Along the scarp, 1306 blocks are mapped, and their volumes (m^3) are estimated (Fig. 4). For lichenometric dating, lichens were measured at 15 stations along the entire scarp (Figs. 2a and 4). To gather them in a group based on their orientation, the main direction of the scarp where each station is located is measured (Fig. 4 and Table 3).

(POSITION OF TABLE 3)

A total of 462 data points were collected for *Aspicilia calcarea*, with diameters ranging from 2.35 mm to 217.71 mm, which are linked to the 2005 and 1089 calendar ages, respectively. We measured 234 lichens of *Aspicilia calcarea* for Group A orientations (at 9 stations), 42 lichens for Group B (at 2 stations), and 186 lichens for Group C (at 4 stations) (Figs. 2a, 4 and Table 3).

(POSITION OF FIGURE 4)

4.1. Correlation of lichen ages and dates of historical earthquakes

An increase in the number of lichens was observed in the 10 years immediately after the occurrence of a historical earthquake. This finding reveals the correlation between the frequency of lichens for calendar age

and the occurrence of historical earthquakes (Fig. 5). This trend is remarkable in Group A after the earthquakes of 1674, 1818, and 1872. Group B is relevant after the earthquakes of 1872 and 1932, while in Group C, this trend is noteworthy after the 1783 and 1855 earthquakes. In the 2011 earthquake, the ecesis period of 10 years and the small diameter of new lichens prevented the increase in the frequency of lichens after this event (Fig. 5). It is remarkable how the lichenometric technique allows us to identify earthquakes that are even more ancient than the documented catalog (1089, 1357 and 1467) (Fig. 5).

(POSITION OF FIGURE 5)

4.2. Rockfall orientation patterns

Each historical earthquake seems to follow a rockfall pattern depending on the groups based on orientation (Fig. 6 and Table 2). For Group B (56°-97°), the peaks of mobilized volume are observed in the 1872 (300 m^3) and 1907 (224 m^3) Totana earthquakes. For scarp segments of Group C (97°-150°), the 1855 Librilla earthquake mobilized the highest rockfall volume (1362 m^3). No specific earthquakes are responsible for the rockfalls for the Group A orientation, although the historical earthquake of 1089 mobilized 630 m^3 of rock (Fig. 6). The rockfall volume per earthquake in Figure 6 is weighted according to the total rockfall volume of each group based on orientation: 1997.75 m^3 (Group A), 533 m^3 (Group B) and 1694.8 m^3 (Group C).

(POSITION OF FIGURE 6)

The rockfall pattern orientation could be controlled by the location of the historical earthquake (Figs. 1, 6 and 7). An example is the Lorca earthquakes of 1674, 1713, 1783, 1818, and 1932, which follow the same orientation pattern of Group A and Group C (Fig. 6). This is also the case for the Totana earthquakes of 1872 and 1907 with dominant rockfall orientations of Group B (56°-97°). The Lorca earthquakes of 1963 and 2011 reflect an orientation pattern similar to that of Group A (Figs. 6 and 7).

In addition, this technique allows the identification of other historical earthquakes that could affect the region. The likely historical earthquakes of 1089 and 1357 created rockfalls in the orientation of 0°-32° (Group A). A possible historical earthquake of 1467 caused rockfalls in the orientation of 97°-150° (Group C) (Figs. 6 and 7).

(POSITION OF FIGURE 7)

4.3. Influence of the rock structure on the rockfall volume.

The vulnerability of the scarp to rockfalls depends not only on its orientation and height but also on its internal structure, which is controlled by the orientation of faults and fractures. The orientation of dominant fractures in the segments and the angles of these fractures based on the orientation of the segment control the size and shape of the blocks of rock susceptible to falling on the slope (Fig. 8). The longer segments are

parallel to the dominant fracture families. The rockfall block volume on the hillslope is analyzed according to the main fracture orientation per segment (Figs. S.1 to S.4). The outcomes show two maximum volumes of fallen rocks in segments oriented N20°-N40° and N80°-N100°. A large rockfall volume ranging from N110° and N130° is remarkable (Fig. 8a). Considering the orientation in Groups A, B and C, the segments oriented 0°-32° and 97°-150° release 40% and 47%, respectively, of the rockfall volume. Group B (56°-97°) releases only 13% of the rockfall volume (Fig. 8b).

(POSITION OF FIGURE 8)

5. DISCUSSION

5.1. Correlation of lichen ages and dates of historical earthquakes

Rockfalls are observed along the Sierra de la Tercia (NE of Lorca), in the northern Sierra de las Estancias (NW of Lorca), and along the Cejo de Cano scarp, which is related to the 2011 earthquake (Rodríguez-Peces et al. 2012; 2020). In this location, there were at least two rockfalls triggered by the 2011 earthquake, and the existence of older rockfalls in its hillslopes could suggest a possible seismic origin behind these rockfalls. To test this hypothesis, lichenometry dating is applied.

The earthquakes of 1674, 1818, and 1872 (Group A) are consistent with the frequency peaks of *Aspicilia calcarea* at 1680-1700, 1820-1840, and 1880-1900, respectively. This trend repeats for the earthquakes of 1872 and 1932 in Group B (1880-1900 and 1940-1950, respectively) and 1783 and 1855 in Group C (1790-1820 and 1860-1880, respectively). Therefore, all these peaks in the frequency of *Aspicilia calcarea* growth are related to several historical earthquakes, which reinforces the induced earthquake hypothesis. A clear correlation is observed between the increase in the frequency of the growth of *Aspicilia calcarea* and the occurrence of historical earthquakes, which demonstrates the reliability of the lichenometric dating technique (Fig. 4). This link between earthquakes and lichen growth that developed on fresh rock rockfall surfaces suggests a likely seismic origin behind the instabilities. In addition, prior lichenometric research conducted at a smaller site in Lorca, which included *Aspicilia calcarea* lichens, obtained a clear association between fallen rocks on hillslopes and the historical earthquakes of 1674 and 1755 (Pérez-López et al. 2012a, 2012b). Due to the correlation of rockfalls in this research with the 1674 and 1755 earthquakes in the literature, the results support the likely seismic origin of the rockfalls in the Cejo de Cano scarp. An important part of this research is a large amount of rockfall-earthquake correlation (Fig. 5) to which the lichenometric technique is applied compared to prior lichenometric studies in the literature.

Despite the longer time frame, a gradual increase in lichen frequency is observed after the 1579 and 1674 earthquakes. For some rockfalls of historical earthquakes of XVIII century and later, mainly on XX century, more data have been collected, so *Aspicilia calcarea* outcomes are more suitable. This is consistent with the complex survival of ancient lichens, which are prone to disappear due to physico-chemical processes and intra- and interspecific competence (Armstrong and Welch, 2007; Rosenwinkel et al. 2015). Despite the shortage of older lichens (<200 yr), more ancient lichens are dated than in the regional historical catalog:

1089, 1357, 1363, and 1467 (Fig. 5). A possible seismic source triggering lichen colonization could be considered.

5.2. Rockfall orientation patterns

The analysis of rockfall orientation patterns shows a correlation with the location of the assigned earthquakes. Thus, the Totana 1872 and 1907 earthquakes show a pattern where Group B is dominant, and the Lorca 1674, 1713, 1783, 1818, and 1932 earthquakes show similar patterns in which Groups A and C are dominant (Fig. 6). Moreover, the Librilla 1855 earthquake shows an orientation pattern that is completely different from that of the other earthquake locations (Totana and Lorca). These results indicate that the location of the earthquakes controls the orientation and volume of the main rockfalls (Figs. 2, 6, and 7). Even though a rockfall orientation pattern based on the location of epicenters is observed, the reason is unknown, and more research related to accelerations and site effects is necessary in the future.

5.3. Influence of the rock structure

The scarps do not have the same vulnerability to rockfalls along their length. They are conditioned by their orientation and the characteristic geometry and size of the rock fracturing (Fig. 7) (e.g., Sago et al. 2007; Martínez-Díaz et al. 2012c; Meunier et al. 2013; Li et al. 2022). The study scarp is highly sensitive to the rockfalls associated with earthquakes due to the high density of scarp-parallel and oblique fracturing. In the Cejo de Cano, two peaks of rockfall volume are obtained in segments oriented N20°-N40° and N80°-N100° (Fig. 8a). The high rockfall volume from N110° to N130° is also remarkable (Fig. 8a). The pie chart accounts for the 0°-32° and 97°-150° orientations encompass 87% of rockfalls and are considered the most expected block drop orientations (Fig. 8b). Consequently, the fracture families of N20°-N40° and N80°-N100°, along with the fracturing between N110° and N130°, determine the orientation prone to the largest rockfalls of 0°-32° and 97°-150°. Hence, the mechanical anisotropy induced by the internal fracturing of rock controls the scarp orientation, which generates the maximum rockfall material. This result has important implications because it provides an approach to the segments that are more likely to produce higher volumes of rockfalls. The study of Harp and Jibson (1996) indicates that a large database could allow quantitative modeling of the relationship between earthquakes, landslide susceptibility, and landslide distribution. Therefore, this study observes how the fracture orientation of the scarp controls the directions of rockfall volumes, which opens up a new field of work for analyzing this type of correlation in larger areas.

6. CONCLUDING REMARKS

A correlation between historical earthquakes and lichen growth developed on fresh rockfall surfaces is observed. This relation indicates a seismic source as a trigger of the rockfalls in the study area. The importance of this study is the large number of earthquakes that correlate with the frequency of lichens compared to studies in the literature.

Even with the high mortality rate of older lichens (<200 yr), more ancient lichens than in the historical catalog are dated in the region. Lichens formed in 1089, 1357, 1363 and 1467 are measured. A possible

seismic source triggering lichen colonization is likely to be considered because they could be linked to the 1089, 1357 and 1467 earthquakes. This study proposes an extension of the regional seismic catalog based on the oldest lichens compared to the documented catalog of historical earthquakes.

The earthquakes located in the same area provoke similar rockfall patterns, as in the case of the Lorca and Totana earthquakes. Although the ultimate cause is not entirely clear, a relationship is observed between the rockfall orientation pattern and the position of the epicenters.

Not only the orientation of a scarp but also the orientation of the fractures affecting the rocks along it is responsible for the direction of rockfall material. In the study region, a high rockfall volume in the N20°-N40° and N80°-N100° orientations, together with the fracturing between N110° and N130°, determine the orientation prone to the largest rockfalls oriented N–S to NNE–SSW and NW–SE. These results show the correlation between the fracture orientation of the scarp and the direction of rockfall volumes, which should be analyzed in the future in larger areas.

REFERENCE LIST

Alfaro, P. Delgado, J. García-Tortosa, F.J. Lenti, L. López J.A, López-Casado, C., Martino, S. (2012). Widespread landslides induced by the Mw 5.1 earthquake of 11 May 2011 in Lorca, SE Spain. *Eng Geol*, 137–138:40–52.

Armstrong, R., Welch, A. (2007). Competition in lichen communities. *Symbiosis*, 43: 1-12.

Benedict, J. B. (1967). Recent glacial history of an alpine area in the Colorado Front Range, U.S.A. 1. Establishing a lichen growth curve. *J. Glaciol.*, 6: 817–832.

Bommer, J.J., Rodríguez, C.E. (2002). Earthquake-induced landslides in Central America. *Eng. Geol.*, 63:189–220

Brune, J.N. (1996). Precariously Balanced Rocks and Ground-Motion Maps for Southern California. *Bull. Seismol. Soc. Am.*, 86: 43-54.

Bull, W.B. (2003). Lichenometry dating of coseismic changes to a New Zealand landslide complex. *Ann. Geophys.*, 46:5.

Bull, W.B., Brandon, M.T (1998). Lichen dating of earthquake-generated regional rockfall events, Southern Alps, New Zealand, *Geol. Soc. Am. Bull.*, 110: 60-84.

Bull, W.B. (1996a). Dating San Andreas Fault earthquakes with lichenometry, *Geology*, 24, 111-114.

Bull, W.B (1996b). Prehistorical earthquakes on the Alpine Fault, New Zealand, *J. Geophys. Res*., 101 (B3), 6037-6050.

Bull, W.B., King, J., Kong, F., Moutoux, T., Phillips, W.M. (1994). Lichen dating of coseismic landslide hazards in alpine mountains. *Geomorphology*, 10: 253-264.

Chueca-Cía, J., Julián-Andrés, A. (1995). Datación en depósitos de derrubios gravitatorios a partir de técnicas liquenométricas (Alta Ribagorza, Pirineo oriental oscense*). Lucas Mallada, Revista de Ciencias*, 7: 115-145.

Chueca-Cía, J. (1991). Pautas de flujo en un glaciar rocoso activo (Skjoldalur, Islandia): aplicación de técnicas liquenométricas. En: *Cuadernos I. Geográfica.* Logroño, 47-67.

Crespo-Martín, C., Martín-González, F., Lozano, G. (2018). Revisión y ampliación del catálogo sísmico del noroeste de la Península Ibérica previo a 1755 y sus implicaciones en la actividad intraplaca. *Estudios Geológicos*, 74, e085:1-32. https://doi.org/10.3989/egeol.43083.477

Delano, J. E., Gold, R. D., Briggs, R. W., and Jibson, R. W. (2018). Coseismic sackungen in the New Madrid seismic zone, USA. *Geophysical Research Letters*, vol. 45 https://doi.org/10.1029/2018GL080493

Delgado, J., Rosa, J., Peláez, J.A., Rodríguez-Peces, M.J., Garrido, J., Tsige, M. (2020). Newmark displacement data for low to moderate magnitude events in the Betic Cordillera. *Data Br.*, 32: 106097.

Echeverría, A., Khazaradze, G., Asensio, E., Gárate, J., Martín-Dávila, J., Suriñach, E. (2013). Crustal deformation in Eastern Betics from CuaTeNeo GPS network. *Tectonophysics*, 608: 600–612.

Garibotti, I.A., Villalba, R. (2009). Lichenometric dating using Rhizocarpon subgenus Rhizocarpon in the Patagonian Andes, Argentina. *Quat. Res.*, 71: 271-283.

Guemache, M.A., Machane, D., Beldjoufi, H., Gharbi, S., Djadia, L., Benahmed, S., Ymmel, H. (2010). On a damaging earthquake-induced landslide in the Algerian Alps: the March 20, 2006 Laâlam landslide (Babors chain, northeast Algeria), triggered by the Kherrata earthquake (Mw = 5.3). *Natural Hazards*: 54, 273-288. https://doi.org/10.1007/s11069-009-9467-z

Guidoboni, E., Ebel, J.E. (2009). *Earthquakes and Tsunamis in the Past: A Guide to Techniques in Historical Seismology*. Cambridge University Press.

Harp, E.L., Jibson, R.W. (1996). Landslides Triggered by the 1994 Northridge, California, Earthquake. *Bull. Seismol. Soc. Am.*, 86: 319-332.

Harp, E.L., Jibson R. W. (2002). Anomalous Concentrations of Seismically Triggered Rock Falls in Pacoima Canyon: Are They Caused by Highly Susceptible Slopes or Local Amplification of Seismic Shaking? *Bull. Seismol. Soc. Am.*, 92 (8): 3180–3189. https://doi.org/10.1785/0120010171

Hughes, P.D (2007). Recent behavior of the Debeli Namet glacier, Durmitor Montenegro. *Earth Surf. Process. Landf.*, 32: 1593-1602.

IGME (2023). QAFI: Quaternary Active Faults Database of Iberia. Data accessed from IGME website: https://info.igme.es/QAFI

IGN (2023). Catalogue of the most relevant earthquakes. Data accessed from IGN website: https://www.ign.es/web/ign/portal/terremotos-importantes

Jomelli, V., Grancher, D., Naveau, P., Cooley, D., y Brunstein, D. (2007). Assessment study of lichenometric methods for dating surfaces. *Geomorphology*, 86:131-143.

Koukouvelas, I. Litoseliti, A. Nikolakopoulos, K. Zygouri, V. (2015). Earthquake triggered rock falls and their role in the development of a rock slope: The case of Skolis Mountain, Greece. *Eng. Geol.*, 191: 71-85. https://doi.org/10.1016/j.enggeo.2015.03.011

Li, N., Tang, C., Yang, T. (2022). Ten years of landslide development after the Wenchuan earthquake: a case study from Miansi town, China. *Natural Hazards*, 111: 2787-2808. https://doi.org/10.1007/s11069-021-05157-y

519 Lin, C.W., Shieh, C.L., Yuan, B.D., Shieh, Y.C., Liu, S.H., Lee, S.Y. (2003). Impact of Chi-Chi
520 earthquake on the occurrence of landslides and debris flows: example from the Chenyulan River
521 watershed Nantou, Taiwan. *Eng Geol*, 71:49–61

522 Martín-González, F. (2018). Earthquake damage orientation to infer seismic parameters in archaeological
523 sites and historical earthquakes. *Tectonophysics*, 724–725: 137–145.
524 https://doi.org/10.1016/j.tecto.2018.01.013

525 Martín-González, F. (2021). Review and Proposed Method to Study the Damage Orientation of Earthquake
526 Effects in Pre-Instrumental Earthquakes. *Izv., Phys. Solid Earth*, 57: 980–993
527 https://doi.org/10.1134/S1069351321130012

528 Martino S., Fiorucci M., Marmoni G. M., Casaburi L., Antonielli B., Mazzanti P. (2022). Increase in
529 landslide activity after a low-magnitude earthquake as inferred from DInSAR interferometry. *Scientific*
530 *Reports*. 12: 2686

531 Martínez-Díaz, J.J., Álvarez-Gómez, J.A., García-Mayordomo, J.M., Insúa-Arévalo, J.M., Martín-
532 González, F, Rodríguez-Peces, M.J. (2012a). Interpretación tectónica de la fuente del terremoto de
533 Lorca de 2011 (M_w 5,2) y sus efectos arquitectónicos. *Revista de Ciencias de la Tierra, Boletín*
534 *Geológico y Minero* 123, 441-458.

535 Martínez-Díaz, J.J., Masana, M., Ortuño, M. (2012b). Active tectonics of the Alhama de Murcia fault, Betic
536 Cordillera, Spain. *J. Iber. Geol.*, 38, 253-270.

537 Martínez-Díaz, J.J., Bejar-Pizarro, M., Álvarez-González, J.A., Mancilla, F., Stich, D., Herrera, G.,
538 Morales, J. (2012c). Tectonic and seismic implications of an intersegment ruptura. The damaging May
539 11th 2011 Mw 5.2 Lorca, Spain, earthquake. *Tectonophysics*, 546-547: 28-37.

540 Martínez-Solares, J.M., Mezcua Rodríguez, J. (2002). *Catálogo sísmico de la Península Ibérica (880 a. C-*
541 *1900).* Dirección General del Instituto Geográfico Nacional, Madrid, 256 p.

542 Matthews, J.A. (2005). "Little Ice Age" glacier variations in Jotunheimen, southern Norway: a study in
543 regionally controlled lichenometric dating of recessional moraines with implications for climate and
544 lichen growth rates. *The Holocene*, 15: 1-19.

545 McCarthy, D.P. y Smith, D.J. (1995). Growth Curves for Calcium-tolerant Lichens in the Canadian Rocky
546 Mountains. *Arctic and Alpine Research*, 27(3): 290-297.

547 Meunier, P., Uchida, T., Hovius, N. (2013). Landslide patterns reveal the sources of large earthquakes.
548 *Earth Planet. Sci. Lett.*, 363: 27–33

549 Musson, R. (1996). Determination of parameters for historical British earthquakes. *Annali di Geofisica.*,
550 34: 1041-1047

Ortuño, M., Masana, E., García-Meléndez, E, Martínez-Díaz, J.J., Štepancíková, P., Cunha, P., Sohbati, R., Canora, C., Buylaert, J.P. y Murray, A.S. (2012). An exceptionally long paleoseismic record of a slow-moving fault: the Alhama de Murcia fault (Eastern Betic Shear Zone, Spain). *Geol. Soc. Am. Bull.*, 124: 1474-1494.

Pérez-López, R, Giner-Robles, J.L., Rodríguez-Pascua, M.A., Silva, P.G., Roquero, E., Bardají, T., Elez J.,Huerta P. (2019). Lichenometric dating of coseismic rockfall related to the Great Lisbon Earthquake in 1755 affecting the archaeological site of "Tolmo de Minateda" (Spain). *Zeitschrift für Geomorphologie*, 62(2), 271-293.

Pérez-López, R., Martín-González, F., Martínez-Díaz, J.J., Rodríguez-Pascua, M.A. (2012a). Datación mediante liquenometría de los desprendimientos rocosos asociados a la sismicidad histórica en Lorca (Murcia, SE de España). *Boletín Geológico y Minero* 123 (4), 473-485.

Pérez-López, R., Martínez-Díaz, J.J., Rodríguez-Pascua, M.A., Martín-González, F. (2012b). Análisis de sismicidad histórica en Lorca mediante liquenometría aplicada a caídas de bloques: los terremotos de 1579 AD, 1674 AD y 2011. *Geotemas*, vol. 13 pp. 470.

Porter, S.C. (1981). Lichenometric studies in the cascade range of Washington: establishment of *Rhizocarpon geographicum* growth curves at mount rainier. *Artic and Alpine Research*, vol. 13, 1: 11-23.

Rodríguez-Peces, M.J., Román-Herrera, J.C., Peláez, J.A., Delgado, J., Tsige, M., Missori, C., Martino, S., Garrido, J. (2020). Obtaining suitable logic-tree weights for probabilistic earthquake-induced landslide hazard analyses. *Eng.Geol.*, 275: 105743.

Rodríguez-Peces, M.J., García-Mayordomo, J., Martínez-Díaz, J.J. (2014). Slope instabilities triggered by the 11th May 2011 Lorca earthquake (Murcia, Spain): comparison to previous hazard assessments and proposition of a new hazard map and probability of failure equation**.** *Bulletin of Earthquake Engineering*, 12-5: 1961-1976.

Rodríguez-Peces, M.J., García-Mayordomo, J., Martínez-Díaz, J.J., Tsige, M. (2012). Inestabilidades de ladera provocadas por el terremoto de Lorca de 2011 (M_w 5,1): comparación y revisión de estudios de peligrosidad de movimientos de ladera por efecto sísmico en Murcia. *Boletín Geológico y Minero* 123 (4): 459-472.

Rogers, R.W. (1999). Biology of Lichens. PhD, Univ. Adelaide (Australia), 858 p.

Rosenwinkel, S., Korup, O., Landgraf, A. y Dzhumabaeva, A. (2015). Limits to lichenometry. *Quaternary Science Reviews*, 129: 229-238.

Sato, H.P., Hasegawa H., Fujiwara, S., Tobita, M., Koarai M., Une H., Iwahashi J. (2007). Interpretation of landslide distribution triggered by the 2005 Northern Pakistan earthquake using SPOT 5 imagery. *Landslides*, 4(2): 113–122.

Silva, P.G., Goy, J.L. Somoza, L., Zazo, C., Bardaji, T. (1993). Landscape response to strike-slip faulting linked to collisional settings: Quaternary tectonics and basin formation in the Eastern Betics, southeastern Spain. *Tectonophysics*, 224: 289-303.

Vera, J.A. (2004). *Geología de España*. SGE-IGME, Madrid, 884 p.

Xu, C., Xu, X., Yao, X. Dai, F. (2014). Three (nearly) complete inventories of landslides triggered by the May 12, 2008 Wenchuan Mw 7.9 earthquake of China and their spatial distribution statistical analysis. *Landslides* 11(3): 441–461.

Wilkinson, R. (2011). A Multi-Proxy study of Late Holocene environmental change in the Prokletije Mountains, Montenegro and Albania. PhD, Univ. Manchester, 414 p.

Winchester, V. (2023). Lichenometric Dating and Its Limitations and Problems: A Guide for Practitioners. *Land* 12:611. https://doi.org/10.3390/land12030611

Winchester, V. (1984). A proposal for a new approach to lichenometry. *British Geomorphological Research Group Technical Bulletin*. 33: 3-20.

CAPTIONS

Fig. 1 Regional map of the studied region marked as CC (Cejo de Cano) in the black square. Seismicity is marked by colored points according to the intensity. The dates of historical earthquakes are shown in black. The dates and intensities of selected earthquakes (Table 1) are marked in red. Municipalities are represented with gray polygons. Inset: location map of the Iberian Peninsula

Fig. 2 (a) Location of the studied region (Cejo de Cano), NW of Lorca municipality. Yellow line: segments defined in Table 2. Blue circles: studied stations and their names. Red circles: studied stations and their names, with rockslides affected by the 2011 earthquake. Inset: location map of the Iberian Peninsula. (b) Geology of Cejo de Cano and surroundings

Fig. 3 Rockfalls at Cejo de Cano in (a) a general view at the southern of segment 1 (b) at Station 11, and (c) at Station 12, with recent rockfalls (white rocks) of the 2011 Lorca earthquake (Fig. 1). (d) *Aspicilia calcarea* on rocks in the study region

Fig. 4 Rockfalls digitalized for the studied scarp. (a) Rockfalls and stations in southern Cejo de Cano. The dotted box shows a detailed region shown in b. (b) Details of mapped rockfalls in southern segments

Fig. 5 Frequency of *Aspicilia calcarea* lichen for groups based on orientation, with bins of 10 years. (a) Group A (0°-32°). (b) Group B (56°-97°). (c) Group C (97°-150°). Cataloged historical earthquakes marked with colored lines and their years of occurrence on the top (Table 1). Gray boxes depict the ecesis of 10 years in Aspicilia calcarea growth

Fig. 6 (a) Orientation of the volume of rockfall per earthquake compared to the orientation of the total volume of rockfall (see the text for explanation). (b) The directional diagrams proportionally depict the top chart that follows real orientations. Group C orientations are doubled because of the two orientations in the scarp (Figure 7). In the 1977 earthquake, no rocks were mobilized

Fig. 7 Scheme of rockfall patterns of Figure 6 based on the scarp orientation (Groups A, B, and C)

Fig. 8 (a) Volume of rockfall weighted with the segment length versus the fracture orientation. (b) Percentage of the volume of rockfall for each orientation in the Cejo de Cano scarp

STATEMENTS AND DECLARATIONS

Acknowledgments

The authors would like to thank the anonymous reviewers for their valuable comments and recommendations that greatly improved the manuscript quality. The corresponding author expresses her gratitude to the two other authors for all that they have taught her. It is an honor to work with you.

Funding

This work has not received funding.

Competing Interests

The authors have no relevant financial or nonfinancial interests to disclose related to this work.

Author Contributions

The authors José Jesús Martínez Díaz and Fidel Martín González contributed to the conception of this work. Material preparation, data collection, analysis and design were performed by Cristina Crespo Martín, José Jesús Martínez Díaz and Fidel Martín González. The first draft of the manuscript was written by Cristina Crespo Martín, and all authors commented on previous versions of the manuscript. All the authors have read and approved the final manuscript.

Figure 1

Click here to access/download;Figure;Fig 1.eps

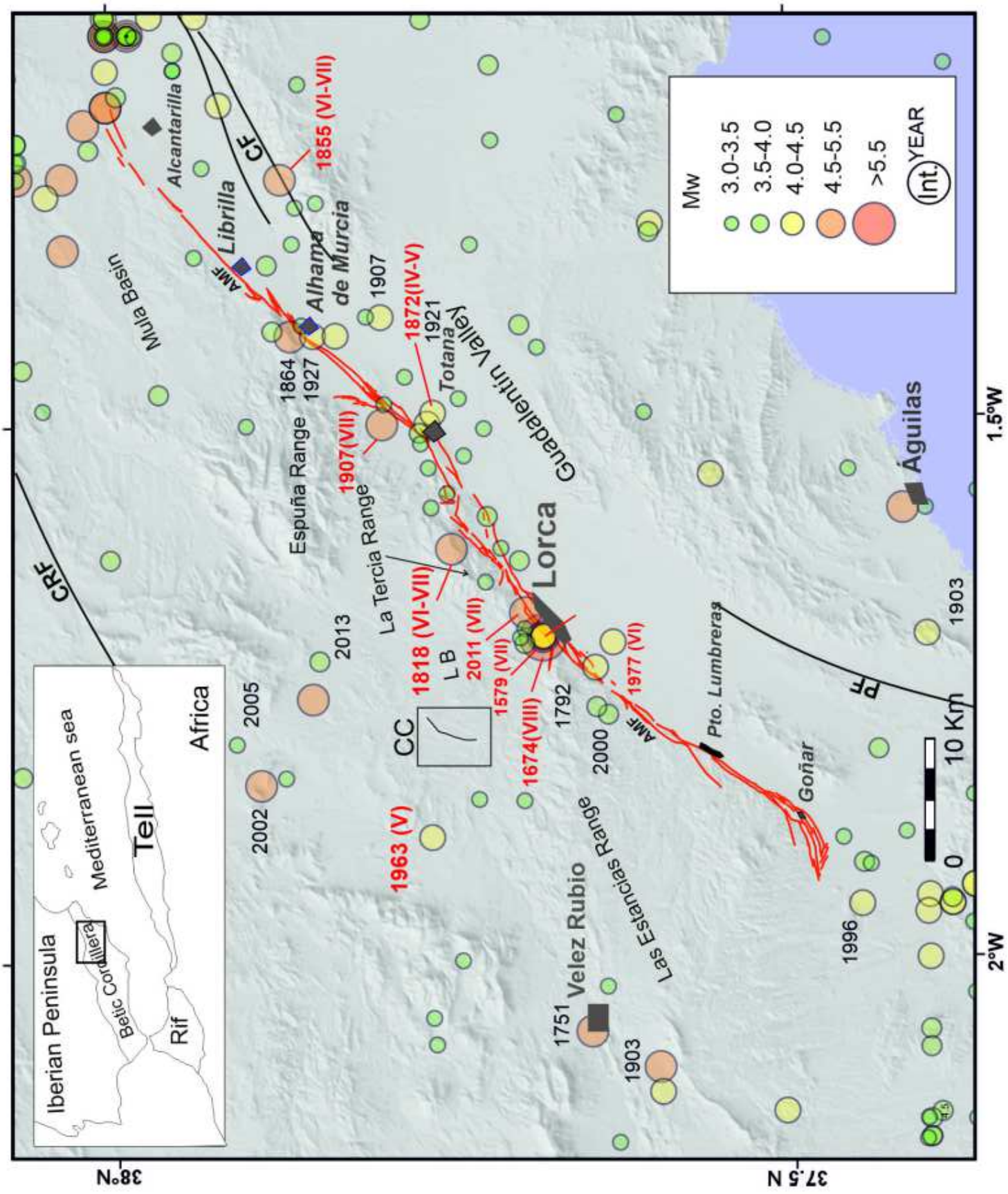

Figure 2

Click here to access/download;Figure;Fig 2.eps

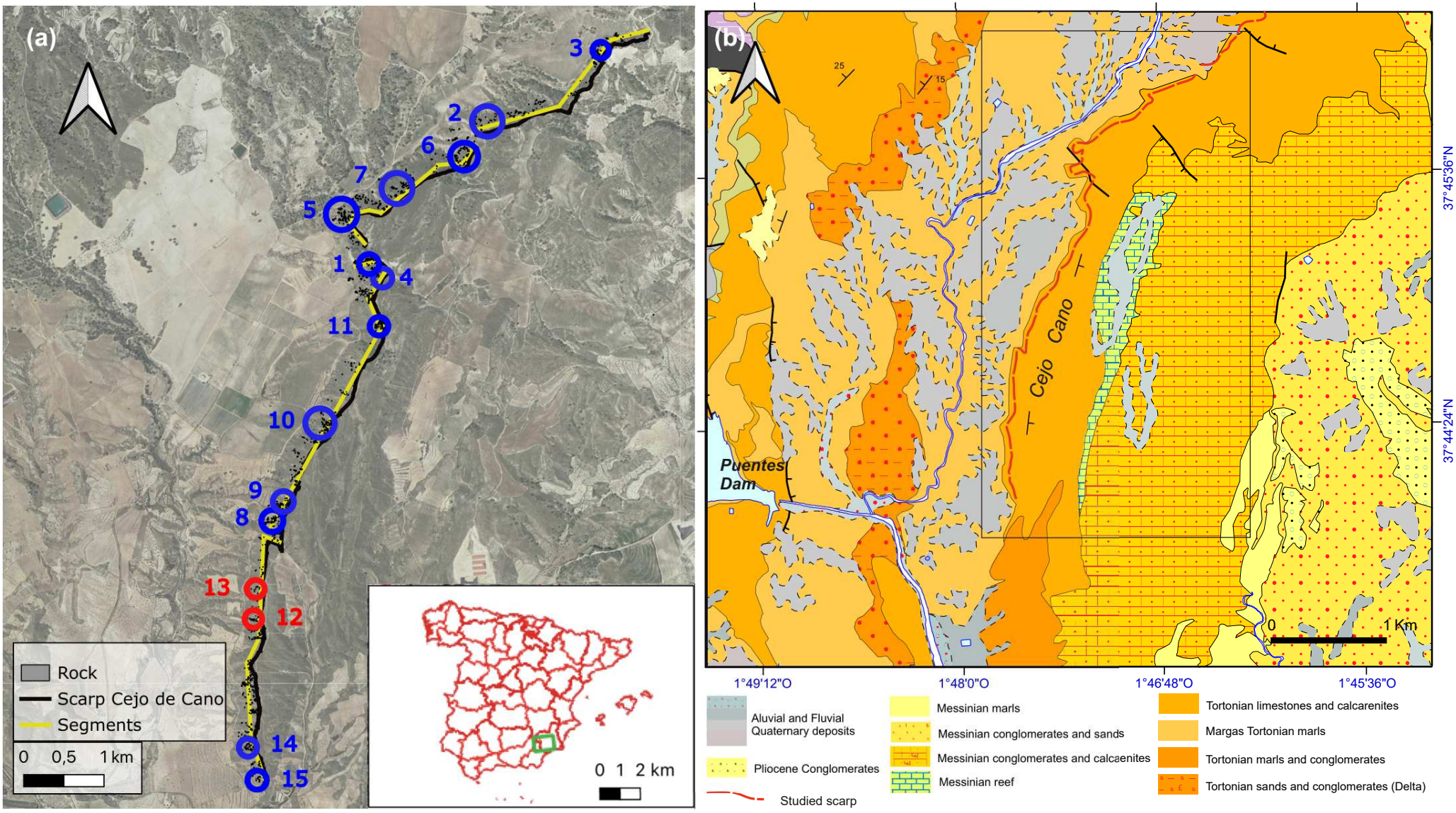

Figure 3

Click here to access/download;Figure;Fig 3.eps

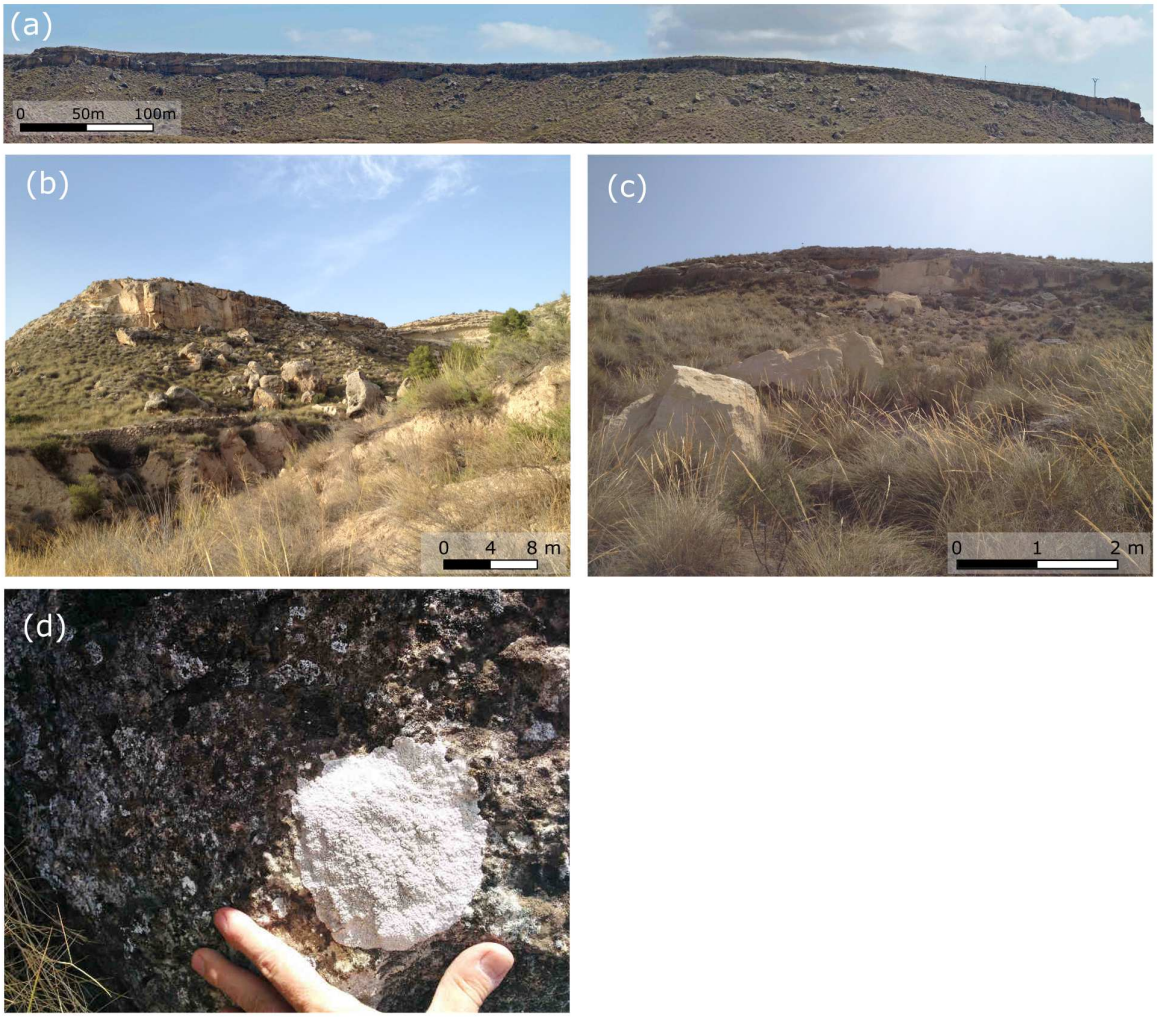

Figure 4

Click here to access/download;Figure;Fig 4.eps

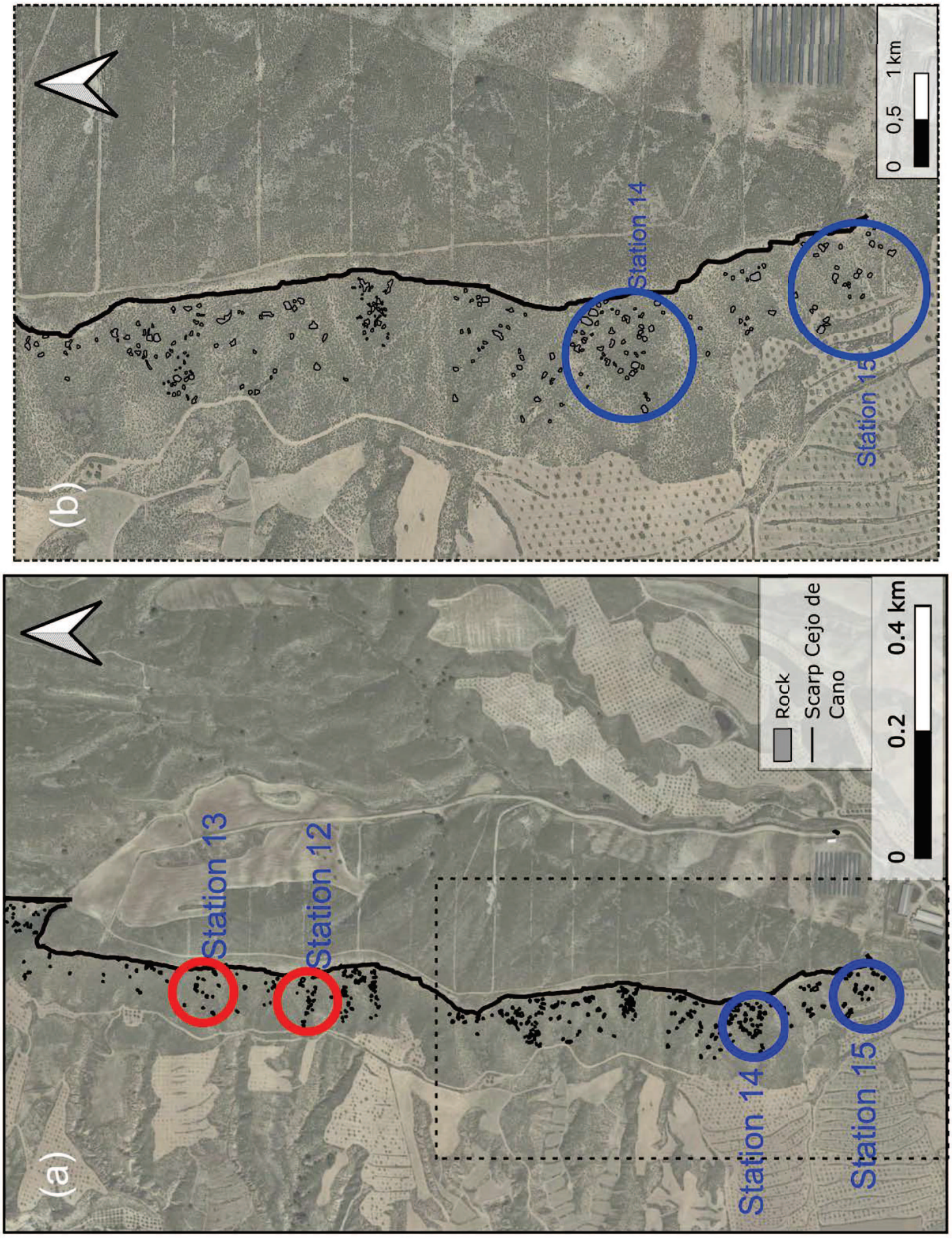

Figure 5

Click here to access/download;Figure;Fig 5.eps

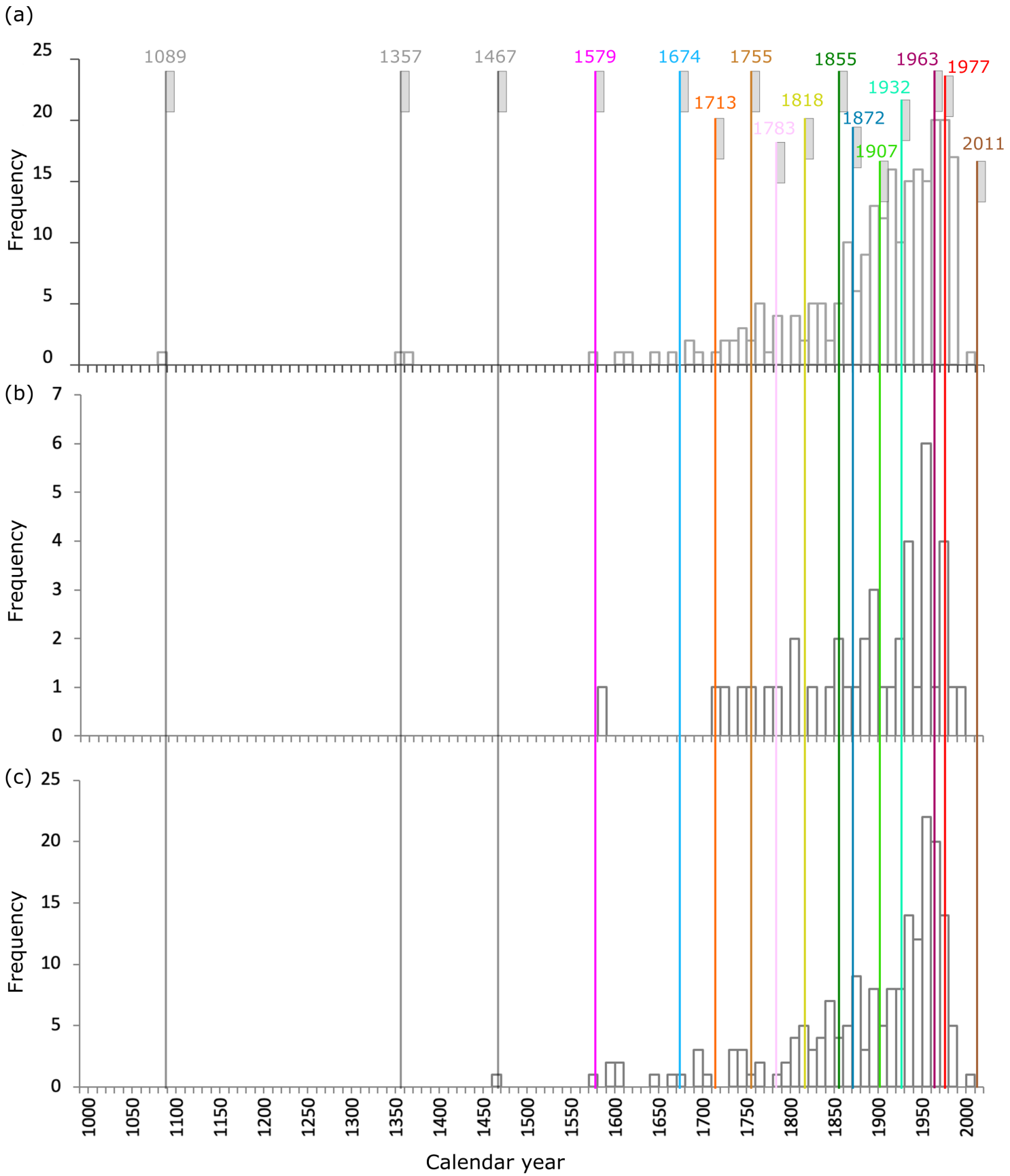

Figure 6

Click here to access/download;Figure;Fig 6.eps

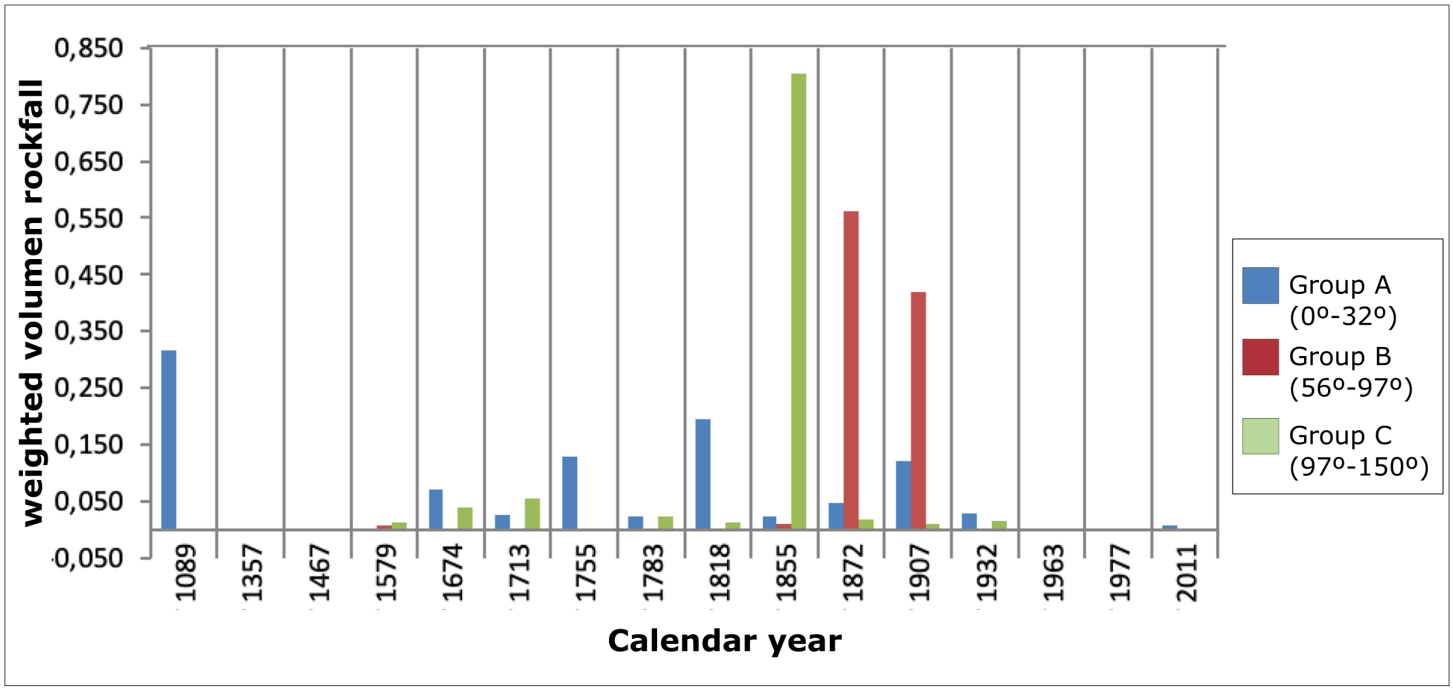

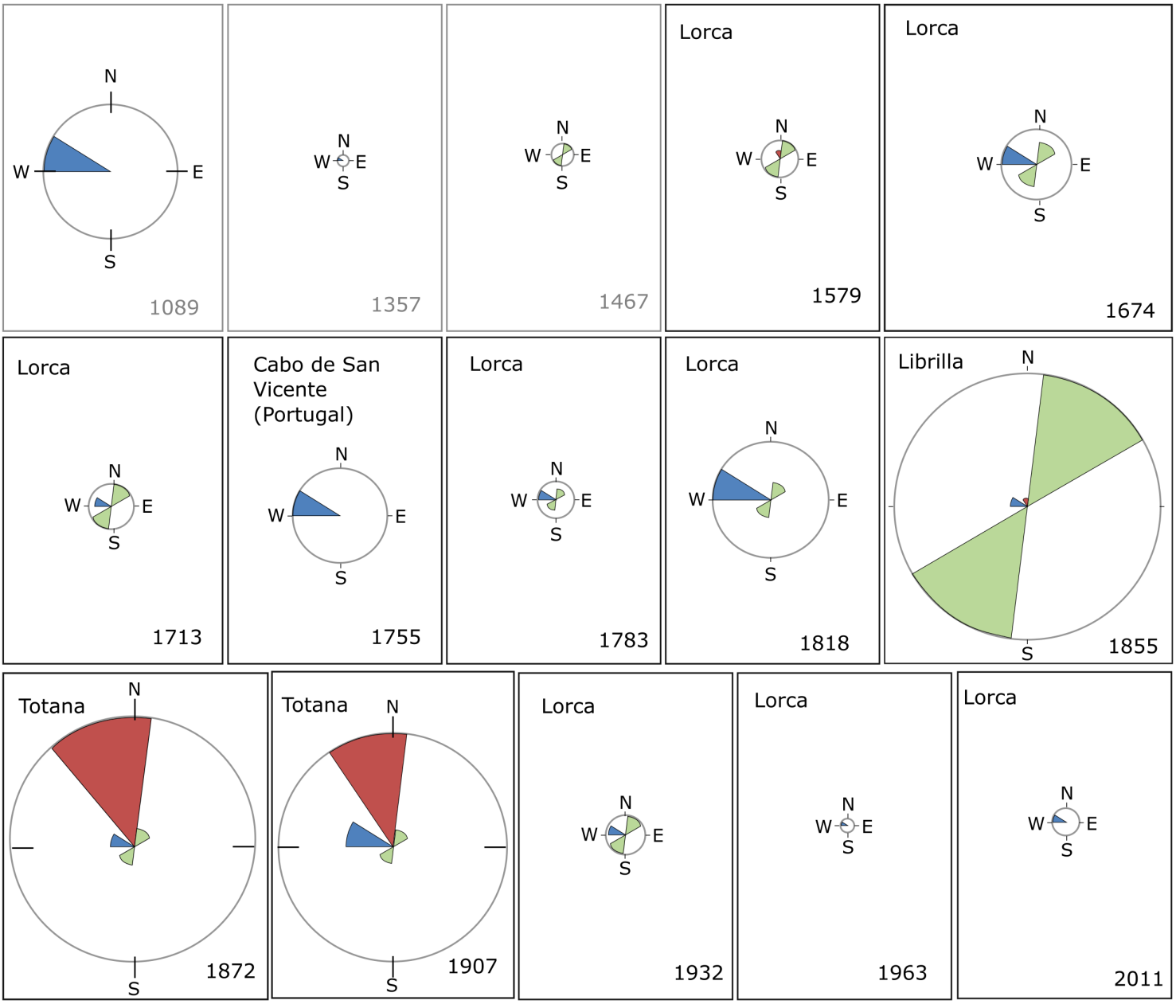

Figure 7

Click here to access/download;Figure;Fig 7.eps

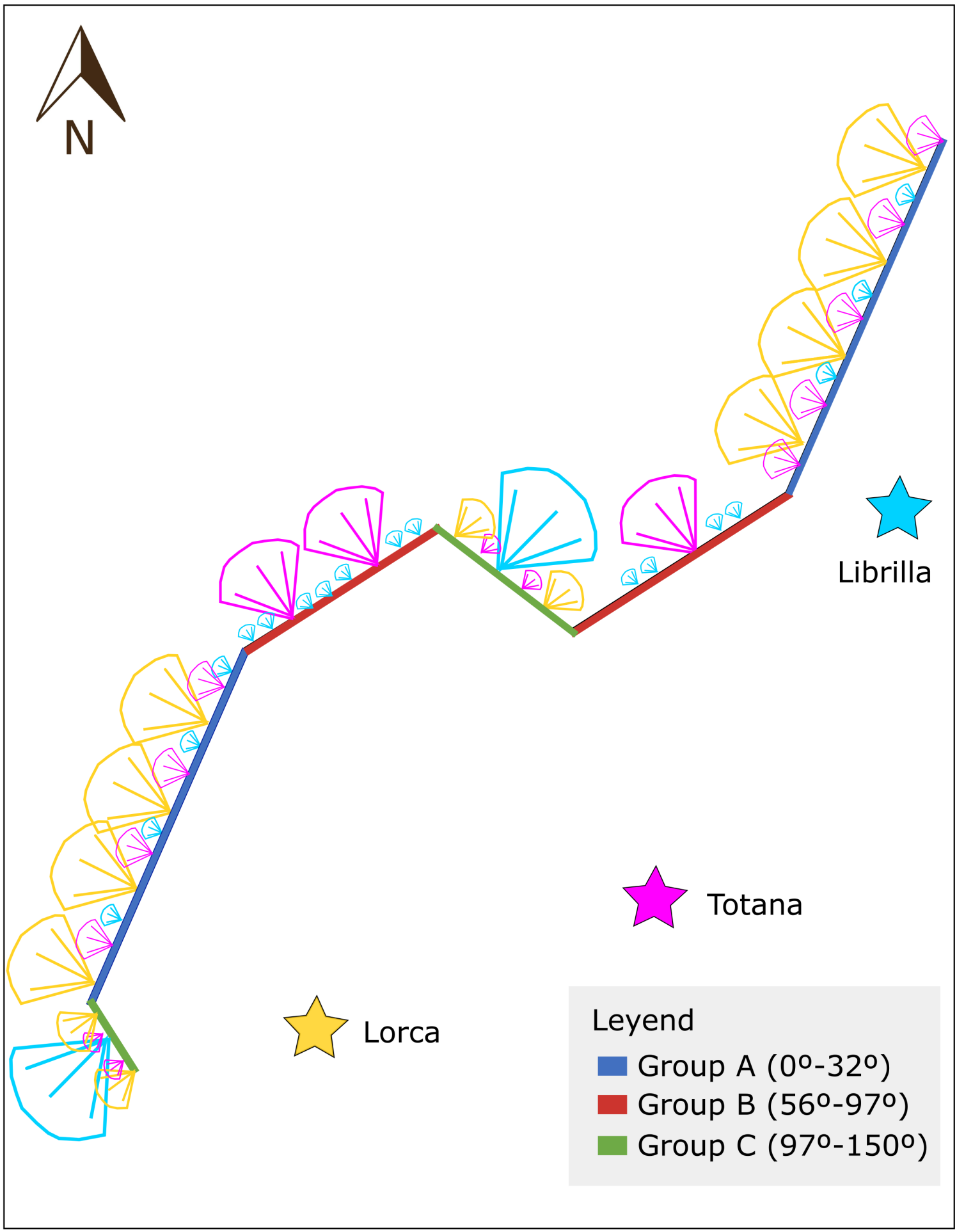

Figure 8

Click here to access/download;Figure;Fig 8.eps

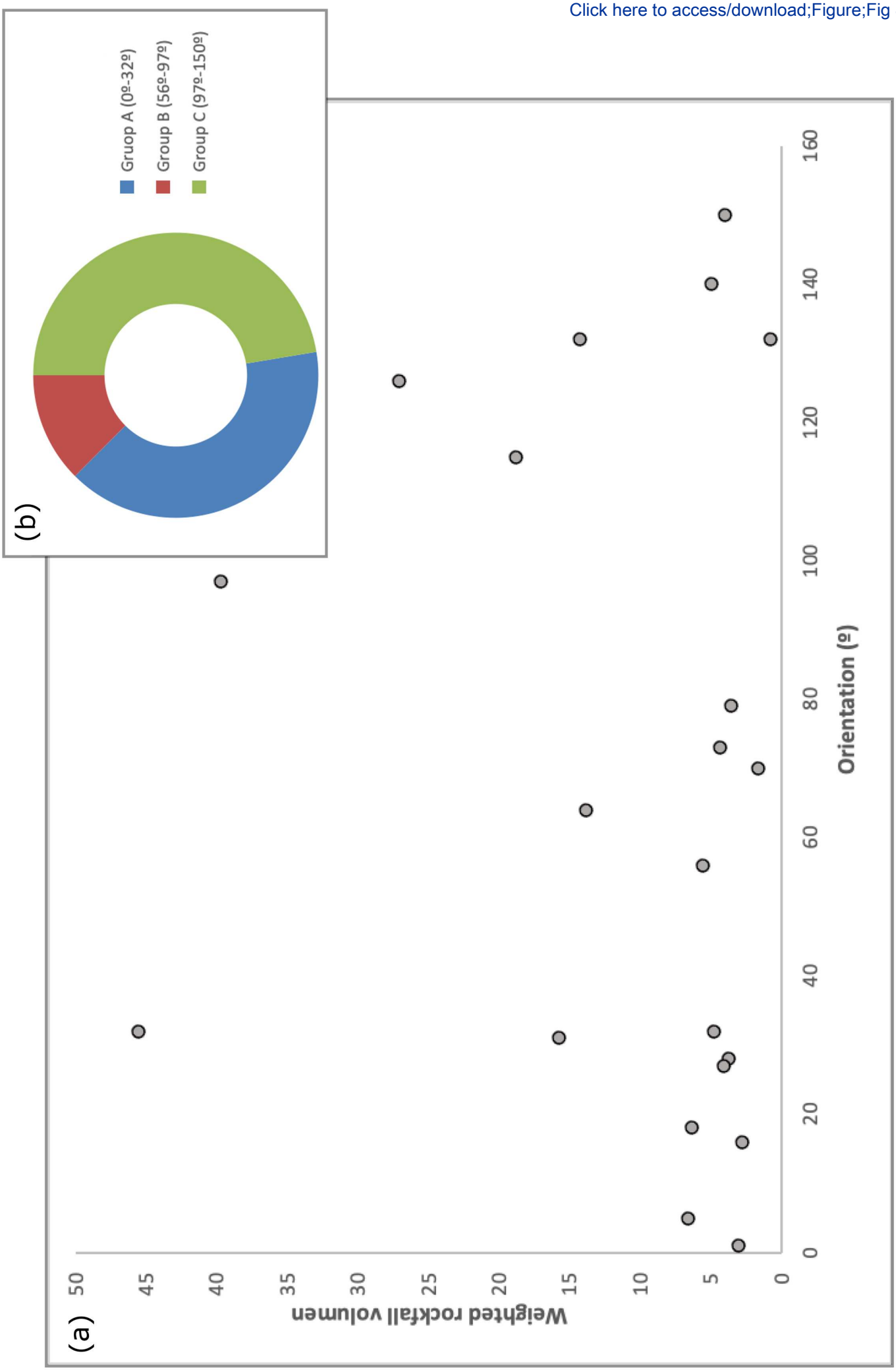

Table 1. Historical and instrumental earthquakes (EMS98< IV) affecting the studied area. Considering the high intensity (≥IV) and nearness of Cejo de Cano, the earthquakes selected for this research are marked in bold. LAT and LONG refer to Latitude and Longitude, respectively. MW: magnitude in Mw. INT: intensity of EMS-98 scale. (Data collected from IGN).

	LAT	LONG	DEPTH	MW	INT	LOCATION
30/01/1579	**37.6833**	**-1.7000**	**0**		**VII**	**Lorca.MU**
28/08/1674	**37.6833**	**-1.7000**	**0**		**VIII**	**Lorca.MU**
03/10/1713	**37.6833**	**-1.7000**	**0**		**IV-V**	**Lorca.MU**
04/03/1751	37.6500	-2.0667	0		VI-VII	Velez Rubio.AL
29/03/1783	**37.6833**	**-1.7000**	**0**		**V-VI**	**Lorca.MU**
16/09/1792	37.6833	-1.7000	0		IV-V	Lorca.MU
20/12/1818	**37.7500**	**-1.6167**	**0**		**VI-VII**	**NE. Lorca.MU**
11/11/1855	**37.8647**	**-1.3147**	**0**		**VI-VII**	**Librilla.MU**
12/01/1864	37.8500	-1.4167	0		V-VI	Alhama de Murcia.MU
21/02/1872	**37.7667**	**-1.5000**	**0**		**IV-V**	**Totana.MU**
24/11/1903	37.6000	-2.1000	0		VI	Velez Rubio.AL
11/02/1907	37.8000	-1.4000	0		V	Alhama de Murcia.MU
16/04/1907	**37.8000**	**-1.5000**	**0**		**VII**	**Totana.MU**
22/01/1921	37.7667	-1.5000	0		V	Totana.MU
24/10/1927	37.8333	-1.4167	0		V	Alhama de Murcia.MU
04/04/1932	**37.6667**	**-1.7000**	**0**		**V**	**Lorca.MU**
23/06/1948	38.0467	-1.7617	5	5.2	VII	SE Cehegín.MU
30/05/1963	**37.7667**	**-1.8850**	**5**	**4.2**	**V**	**NW Lorca.MU**
06/06/1977	**37.6450**	**-1.7283**	**9**	**4.4**	**VI**	**SW Lorca.MU**
22/10/1996	37.4750	-1.8700	1	4.1	V	NE Huércal-Overa.AL
23/08/2000	37.6358	-1.7722	0	4.0	V	SW Lorca.MU
06/08/2002	37.8925	-1.8353	1	5.0	V	SW Bullas.MU
03/02/2005	37.8349	-1.7864	6	4.3	IV-V	NW Lorca.MU
11/05/2011	**37.7175**	**-1.7114**	**4**	**5.1**	**VII**	**NE Lorca.MU**
11/05/2011	37.7196	-1.7076	2	4.5	VI	N Lorca.MU
04/04/2013	37.8247	-1.7870	11	3.7	IV-V	NW Lorca.MU

Table 2. Segments classification in groups based on orientation.

	Orientation (º)		Segments
Group A	N-S to NNE-SSW	0º to 32º	2,3,4,5,7,9,10,14, 19 and 21
Group B	NE-SW	56º to 97º	15,17,18, 20 and 22
Group C	NW-SE	97º to 150º	1,6,8,11,12, 13 and 16

Table 3. Classification of stations in Groups A, B, and C, depending on the orientation.

Station	Main orientation	Orientation(º)		Group
1	125.67	97º to 150º	NW-SE	C
2	73.05	56º to 97º	NE-SW	B
3	31.7	0º to 32º	N-S to NNE-SSW	A
4	131.69	97º to 150º	NW-SE	C
5	38.22	0º to 32º	N-S to NNE-SSW	A
6	30.99	0º to 32º	N-S to NNE-SSW	A
7	55.78	56º to 97º	NE-SW	B
8	13.03	0º to 32º	N-S to NNE-SSW	A
9	19.37	0º to 32º	N-S to NNE-SSW	A
10	22.33	0º to 32º	N-S to NNE-SSW	A
11	96.69	97º to 150º	NW-SE	C
12	5.59	0º to 32º	N-S to NNE-SSW	A
13	12.3	0º to 32º	N-S to NNE-SSW	A
14	8.43	0º to 32º	N-S to NNE-SSW	A
15	140.11	97º to 150º	NW-SE	C